Electrochimica Acta 329 (2020) 135142

Contents lists available at ScienceDirect

Electrochimica Acta

journal homepage: www.elsevier.com/locate/electacta

Synthesis, characterization and electropolymerization of functionalized organic salt—anilinium saccharinate and electrochemically controlled release of saccharinate anions

Lanbo Shen, Na Gao, Xirong Huang*

Key Laboratory of Colloid and Interface Chemistry of the Education Ministry of China, Shandong University, Jinan, 250100, China

ARTICLE INFO

Article history:
Received 15 August 2019
Received in revised form
21 October 2019
Accepted 23 October 2019
Available online 24 October 2019

Keywords:
Functionalized organic salt
Electropolymerization
Conducting polymer
Electrochemically controlled release

ABSTRACT

In this work, a novel functionalized organic salt – anilinium saccharinate ([HANI][Sac]) was synthesized by the ion exchange method, and its composition and properties were characterized by ^{1}H NMR, ^{13}C NMR, ESI/MS and TG-DSC techniques. [HANI][Sac] can be used as both monomer and supporting electrolyte for efficient electrosynthesis of polyaniline (PANI) in acetonitrile. The obtained PANI has hierarchical porous structure and its doping degree with saccharinate anion ($[Sac]^-$) is as high as 33.5%. The resulting $[Sac]^-$-doped-PANI (PANI-[Sac]) can be used as an electrochemically controlled drug delivery system. The *in vitro* release kinetics of $[Sac]^-$ under different potential stimuli conditions showed that, at a given time, the release rate of $[Sac]^-$ and its release percentage (ratio of the amount released to that loaded) increase with the negative shift of the applied potential. The amount of $[Sac]^-$ loaded and/or released can also be regulated by varying the charge for PANI electropolymerization. The present work provides a new strategy for the facile construction of conducting polymer-based electrochemically controlled drug release system.

1. Introduction

Controlled drug release is of great significance for improving drug efficacy and reducing drug side effect [1–3]. As one of the effective ways to control drug release, electrochemically controlled drug release has attracted extensive attention of researchers [4–12]. It is shown that conducting polymer is an excellent carrier for the electrochemically controlled drug release [13–16]. The tested drugs include dexamethasone, methotrexate, saccharinate, *etc*. The mechanism of the conducting polymer-based electrochemically controlled drug release is as follows. During the electrochemical oxidation, the conducting polymer chain loses electrons and is then positively charged, and the resulting positive charges are counterbalanced by the incorporation of anionic drugs as dopants, *i.e.* the drug loading process; the anionic drugs are released from the polymer during the electrochemical reduction, *i.e.* the drug releasing process. The electrochemical doping/dedoping process of the conducting polymer is also accompanied by a change of the polymer volume (swelling/shrinking) [2,5,7,17–19]. Conducting polymer-based electrochemically controlled drug release systems have many advantages: Firstly, some conducting polymers such as polypyrrole and polyaniline (PANI) usually have good electrical conductivity, good environmental stability and good biocompatibility; moreover, they can be facilely in-situ synthesized on conductive substrate (the size could be as small as micrometer) using electrochemical methods (such as cyclic voltammetric, potentiostatic and galvanostatic) with controlled morphologies. Secondly, the amount of drug loaded by conducting polymer is relatively large, for example, the loads of dexamethasone by PEDOT and acesulfame by polypyrrole are estimated to be 2.2 mmol g^{-1} and 1.8 mmol g^{-1}, respectively [4,5]. Finally, the precise and continuous controlled release of drug can be achieved by varying the current and potential applied [6,20–22]. As the dopant must be a mobile ion (usually an anion), this strategy is suitable only for small charged drug molecules, which is the shortcoming of this strategy [5,7,11,15].

Room temperature ionic liquids (RTILs) are liquid organic salts composed of organic cations and organic or inorganic anions at room temperature. They have some unique properties such as low volatility, high conductivity, good thermostability, wide electrochemical window, strong ability to dissolve substances,

* Corresponding author.
E-mail address: xrhuang@sdu.edu.cn (X. Huang).

https://doi.org/10.1016/j.electacta.2019.135142
0013-4686/

designability and so on. Therefore, they are ideal media for electrosynthesis [23–25]. The use of RTIL as medium for the synthesis of conducting polymers could result in conductive materials with both ionic and electronic properties, which is of great significance for the development of functionalized electrode materials and electrochemical devices [26–30]. In recent years, RTILs containing active pharmaceutical ingredients (API-ILs) have aroused interests in pharmaceuticals and biomedicine areas due to their efficacy in improving drug solubility and bioavailability [31–37]. There have been many reports about API-ILs-based drug delivery systems [38–40]. Yasushi Miwa et al. transformed a poorly water-soluble drug – etodolac (a drug for the treatment of arthritis) into a salt in the form of RTIL, which significantly improved its hydrophobicity, hydrophilicity and skin permeability, and therefore improved the efficiency of transdermal drug delivery [41]. Combining API-ILs with conducting polymers could develop new strategies for the construction of conducting polymer-based electrochemically controlled drug release systems. Stephanie Carquigny et al. used API-ILs as supporting electrolyte to synthesize conducting polypyrrole films and studied the potential-controlled release kinetics of active drug anions as dopants. They found that the drug release rate and the amount released could be controlled by varying the applied potentials [5]. However, there are few reports in this field. In order to simplify the construction of drug delivery system, we develop, in the present work, a novel functionalized organic salt – anilinium saccharinate salt ([HANI][Sac]). Its cation is protonated aniline, which can act as monomer for the eletrosynthesis of PANI; its anion is active pharmaceutical ingredient. Using the functionalized organic salt as supporting electrolyte, active drug anion ($[Sac]^-$) doped PANI (PANI-[Sac]) was synthesized by simple electrochemical method. The present strategy can ensure that the aniline electropolymerization goes effectively without an exogenous proton source and that the drug anion is the only doping anion. The resulting PANI has a hierarchical porous structure with the doping degree of 33.5% and the maximum amount of released drug being 3.6 mmol g^{-1} at −1.5 V (*vs.* SCE).

2. Experimental section

2.1. Materials

Aniline (ANI, ≧99.5%), absolute ethyl alcohol, hydrochloric acid (36%), sulfuric acid (H_2SO_4, 98%) were purchased from Sinopharm Chemical Reagent Co., Ltd., China. Acetone was purchased from Laiyang Kangde Chemical Co., Ltd., China. Acetonitrile was purchased from Yuwang Industrial Co., Ltd., China. Sodium saccharinate (Na [Sac], 99%) and DMSO-d_6 were purchased from Sigma-Aldrich. All chemical reagents were of analytical grade. Ultrapure water (18.25 MΩ·cm) was used throughout the experiments.

2.2. Preparation and characterization of anilinium saccharinate salt

The anilinium saccharinate salt ([HANI][Sac]) was prepared by ion exchange between anilinium chloride ([HANI]Cl) and sodium saccharinate (Na [Sac]). The brief steps are as follows:

1) A 27.9 g of aniline (0.3 mol) and an equivalent mole of hydrochloric acid was mixed in a single-necked flask and the mixture was stirred in ice bath for 3 h, followed by drying in a vacuum oven for 24 h, getting a solid [HANI]Cl.
2) The dried Na [Sac] (12.31 g, 60 mmol) (120 °C, 6 h) was mixed with [HANI]Cl (7.78 g, 60 mmol) in 100 mL absolute ethanol as solvent under stirring overnight.
3) The resulting mixture was filtered to remove NaCl and the solvent ethanol was evaporated under vacuum at 60 °C.
4) The solid product obtained above was dissolved in 100 mL acetone under stirring, followed by filtration through an organic filter to remove residual NaCl precipitate. After that, the solvent acetone was removed under vacuum at 60 °C.
5) The resulting product was placed in a vacuum oven at 70 °C for 48 h, getting the pure [HANI][Sac].

The characterization of [HANI][Sac] was made using NMR, ESI/MS and TG/DSC techniques. The ^1H NMR and ^{13}C NMR spectra of [HANI][Sac] (DMSO-d_6 as solvent) were recorded on a Bruker Avance 300 MHz NMR spectrometer. The mass spectrum of [HANI][Sac] (10 mg mL^{-1} in ethanol) was recorded on an Agilent 6510 Q-TOF mass spectrometer (ESI source). The thermogravimetric and differential scanning calorimetry (TG-DSC) analyses were performed on a PerkinElmer STA 8000 thermal analyzer in a temperature range of 30–200 °C (N_2 atmosphere) with a heating rate of 10 °C min^{-1}.

2.3. Electrosynthesis of PANI

At ambient temperature (~25 °C), 4.0 mL of 0.1 M [HANI][Sac] in acetonitrile was used as a medium (the conductivity is *ca.* 3.3×10^{-4} S cm^{-1}) for the electrosynthesis of PANI. Prior to the electrosynthesis, the medium was purged with high purity nitrogen for 20 min. During the electrosynthesis the nitrogen atmosphere was maintained.

The electrochemical polymerization was performed on a CHI660E electrochemical workstation. The three-electrode system was composed of a working electrode (GC disk electrode, 3 mm in diameter), a Pt wire counter electrode, and a saturated calomel electrode (SCE) as reference (all the potentials given in this paper were *vs.* SCE). Prior to use, the GC disk electrode was polished to a mirrorlike surface in the following steps: firstly, polished with 0.5 μm and 0.05 μm Al_2O_3, respectively, then washed with ultrapure water and ethanol, and finally sonicated in ultrapure water for 5 min. The electrochemical polymerization was carried out using cyclic voltammetry. The setting of the parameters for the electrochemical polymerization was described in the figure captions. After the electropolymerization, the obtained PANI/GC electrode was rinsed with ultrapure water and dried for subsequent use.

2.4. Characterization of PANI

The PANI for FTIR and SEM characterizations was electropolymerized in acetonitrile containing 0.1 M [HANI][Sac] according to the procedure described in section 2.3. To facilitate the characterization, a detachable GC electrode (3 mm in diameter) was used as working electrode. After the electropolymerization, the potential was set at 0.6 V (*vs.* SCE) for 10 s. The GC electrode with PANI was rinsed with ultrapure water, and then dried for subsequent characterization. The morphology of PANI was examined using cold field emission scanning electron microscopy (FESEM, ZEISS GeminiSEM 300, Germany). The FTIR spectrum of the PANI was recorded on an FTIR spectrometer (Thermo scientific Nexus 670, America) in an ATR mode. The doping degree of saccharinate anion ($[Sac]^-$) was characterized by the EDS attachment of a cold field emission scanning electron microscopy (FESEM, ZEISS GeminiSEM 300, Germany).

The PANI for electrochemical characterization was obtained in the same way as described above. Here, the polymerization charge was controlled for comparison, and the electropolymerization was stopped at a potential of −0.2 V (*vs.* SCE) for 60 min. The electrochemical characterization of PANI was carried out by cyclic

voltammetry in 1.0 M H_2SO_4 aqueous solution. The PANI/GC was used as a working electrode, a Pt wire as a counter electrode, and a SCE as a reference electrode.

2.5. In vitro release tests of active pharmaceutical ingredients

A detachable GC electrode (1.0 cm^2) was used as the working electrode, and the electropolymerization was carried out in acetonitrile containing 0.1 M [HANI][Sac] according to the electrosynthesis procedures described in section 2.3 (the charge for the electropolymerization was set at 0.52 C cm^{-2}). After the electropolymerization, the potential was set at 0.6 V (*vs.* SCE) for 10 s. The PANI electrode was rinsed with ultrapure water, and dried for subsequent *in vitro* release tests of $[Sac]^-$ anion. The release tests were performed at room temperature by immersing the PANI electrode in 6.0 mL of 0.1 M PBS (pH 7.0) under constant stirring, followed by electrical stimulus (0.5、-1.0 and −1.5 V *vs.* SCE). An aliquot of sample (200 μL) was taken at a regular interval from the system to measure its absorbance at 270 nm. To keep the volume of the system unchanged, 200 μL fresh PBS was added to the system. The amount of drug released was evaluated based on the calibration curve of Na [Sac]. Samples without electrical stimulus were used as controls.

3. Results and discussion

3.1. Preparation and characterization of [HANI][Sac]

Anilinium saccharinate salt ([HANI][Sac]) is prepared by ion exchange between anilinium chloride ([HANI]Cl) and sodium saccharinate (Na [Sac]). The rationale is shown in Scheme 1.

The obtained [HANI][Sac] was characterized by NMR, ESI/MS and TG/DSC techniques. The ^1H NMR spectrum of [HANI][Sac] is shown in Fig. 1A and proton peaks are observed at δ = 10.39 (br, 3H), 7.62 (m, 4H), 7.52 (m, 2H), 7.49 (m, 3H). Due to the coupling and splitting of protons on the benzene ring, it is difficult to differentiate the chemical shifts of respective protons. The ^{13}C NMR spectrum of [HANI][Sac] can remedy this defect. Fig .1B is the ^{13}C NMR and the major peaks are listed as follows: δ = 168.26, 145.86, 135.37, 132.76, 131.96, 131.30, 130.11, 128.17, 123.51, 123.01, 119.52. The assignment of the corresponding peak is shown in Fig. 1B. Fig. 2 is the mass spectra of [HANI][Sac]. The peaks (*m*/*z*) are assigned as follows: ESI(+): 94.06 ($[HANI]^+$), 184.00 ($[Sac]^-+2H^+$), 277.06 ($[HANI]^+$+$[Sac]^- + H^+$); ESI(−): 181.99 ($[Sac]^-$), 275.06 (ANI+$[Sac]^-$).

Fig. 3 is the TG and DSC thermal analysis curves of [HANI][Sac]. It can be seen from the TG curve that the sample is stable over the temperature range of 30–200 °C. The DSC curve indicates that [HANI][Sac] melts at *ca.* 141 °C.

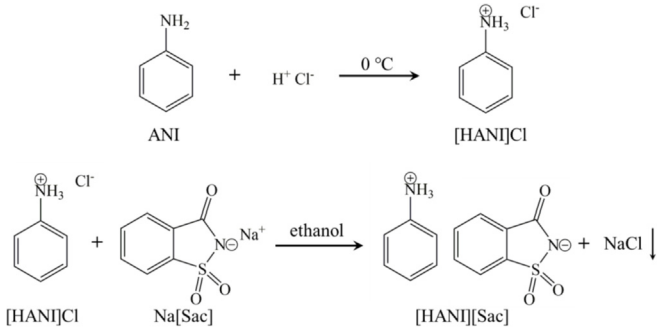

Scheme 1. Preparation of functionalized organic salt [HANI][Sac].

3.2. Electrosynthesis of PANI

The electrosynthesis of PANI was carried out in acetonitrile containing 0.1 M [HANI][Sac]. Fig. 4 shows the cyclic voltammograms (CVs) of the electropolymerization of $[HANI]^+$ on GC working electrode. Two pairs of redox peaks marked as a/a' and b/b' can be seen from Fig. 4. The a/a' should be assigned to the redox process of leucoemeraldine/emeraldine and the b/b' to emeraldine/perniganiline [27,42–45]. With the increase of the scan number, the deposition current, as indicated on the positive end of the scans, decreases first and then levels off. However, the amount of PANI deposited on the electrode, as evidenced by the intercalation currents in Fig. 4, is increased with the cycle number. The change of the increments of the peak currents (a/a' and b/b') per cycle indicates that the rate of PANI growth decreases first and then levels off. The inference made above is supported by the net charge involved in the deposition, which is observed by plotting the integrated current *vs.* time obtained from the cyclic voltammograms (Fig. 5). Fig. 5 shows the overall increment of the amount of the charge passed to deposit PANI is slowed down with increasing the cycle number, which suggests the rate of deposition is slowing. This phenomenon is correlated with the electroactive area of the electrode. At the initial stage, the reacting area of the polymerization is increasing with the amount of polymer. At the later stage, however, the reaction rate will slow as the polymer becomes increasingly dense [29]. The above results indicate that the PANI film can grow steadily in 0.1 M [HANI][Sac] acetonitrile solution.

The potential window is over −0.2–1.0 V. The scan rate is 50 mV s^{-1}.

Fig. 4 also shows that the ΔE_p of a/a' (b/b') increases with increasing the cycle number, indicating that the reversibility of the PANI film becomes worse with the increase of the cycle number. This may be due to the denser PANI film which makes the doping/dedoping of the drug anions become more difficult [46].

3.3. PANI morphology

Fig. 6 is the SEM image of the resulting PANI. It shows that the PANI film has porous structure. The magnified image (inset) indicates that the spindle-like particle is made up of smaller PANI particles. PANI with hierarchical porous structure is an ideal material not only for the fabrication of supercapacitor [47], but also for the construction of electrochemically controlled drug release system.

3.4. FTIR spectroscopy characterization of PANI

Fig. 7 is the FTIR spectrum of the PANI-[Sac] prepared by electropolymerization in 0.1 M [HANI][Sac] acetonitrile solution. The absorption peak at 1660 cm^{-1} is attributed to the stretching vibration of C=O. The peaks at 1552 cm^{-1} and 1454 cm^{-1} are attributed to the characteristic absorption of the quinoid units and the benzenoid units. The absorption peaks at 1367 cm^{-1} and 1294 cm^{-1} are attributed to the C–N stretching vibration of aromatic amines. The absorption at 1242 cm^{-1} is attributed to the $C–N^+$ stretching vibration in the polaron structure. The absorption at 1161 cm^{-1} is assigned to the stretching vibration of S=O. The absorption peaks over a range of 900–700 cm^{-1} is assigned to the characteristic absorption of the aromatic ring with different substituent groups [26,42,48–50]. The FTIR spectrum indicates that the PANI is doped with saccharinate anions. For comparison, the FTIR spectrum of the PANI-Cl is also included in Fig. 7. The PANI-Cl was prepared by electropolymerization of ANI in 0.1 M HCl aqueous solution. As we can see, the two spectra are similar but not identical due to the presence of different doping ions.

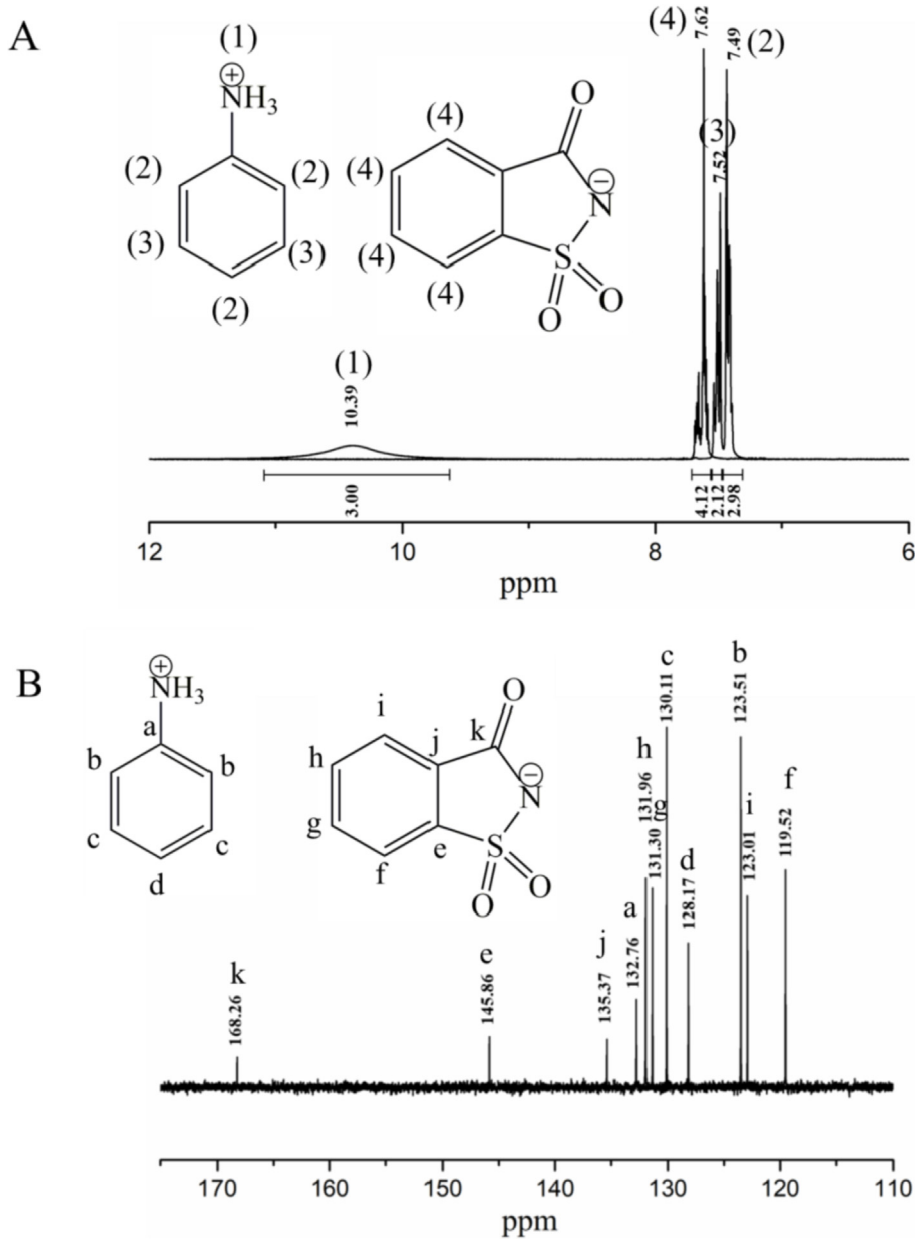

Fig. 1. ^{1}H NMR spectrum (A) and ^{13}C NMR spectrum (B) of [HANI][Sac].

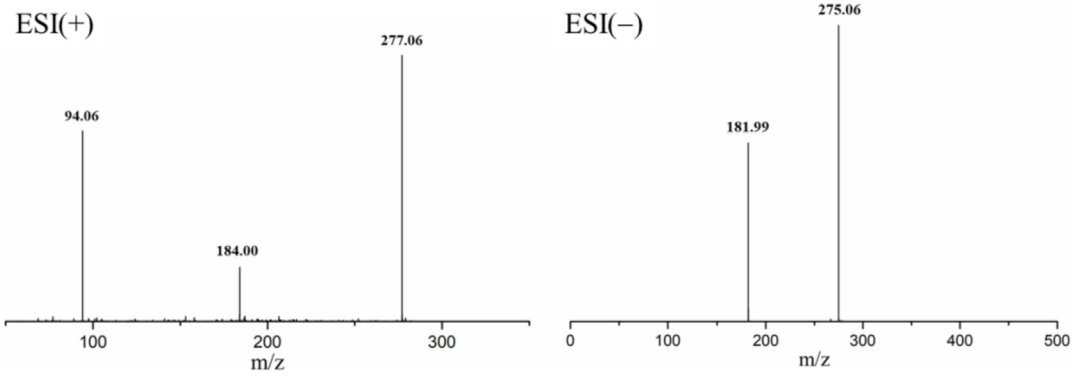

Fig. 2. ESI/MS spectrum of [HANI][Sac].

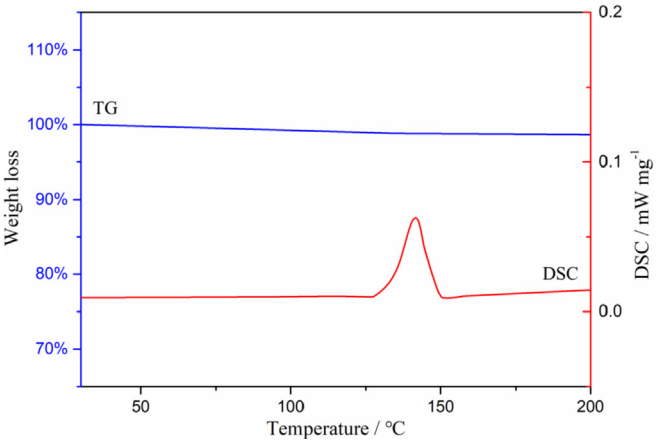

Fig. 3. TG/DSC curve of [HANI][Sac].

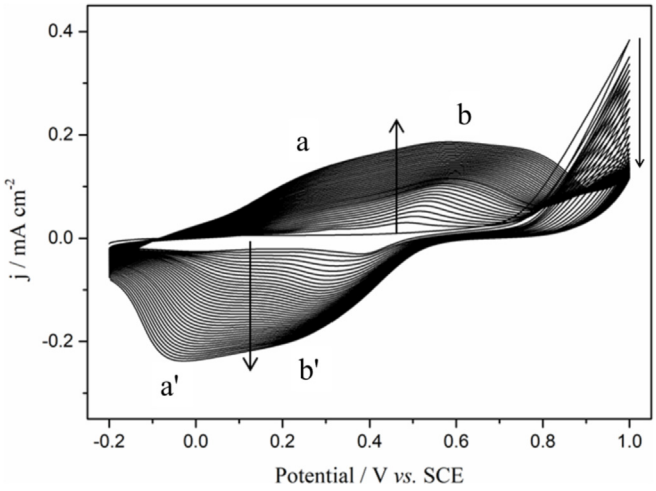

Fig. 4. Cyclic voltammograms in acetonitrile containing 0.1 M [HANI][Sac].

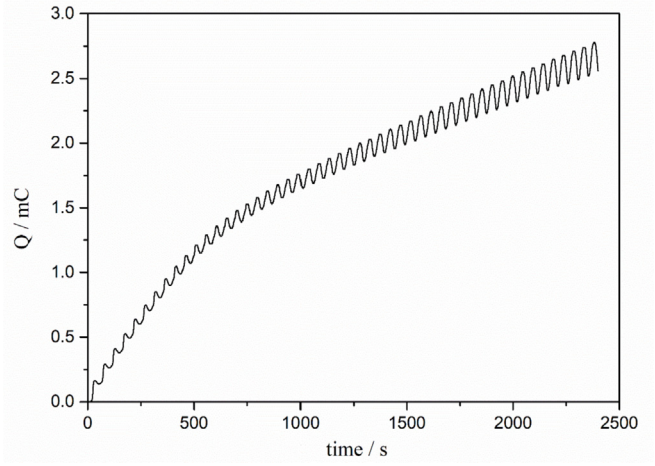

Fig. 5. Charge passed during the deposition of PANI in acetonitrile containing 0.1 M [HANI][Sac] at GC disk working electrode (3 mm in diameter) by cycling 50 times between −0.2–1.0 V. with the scan rate of 50 mV s^{-1}.

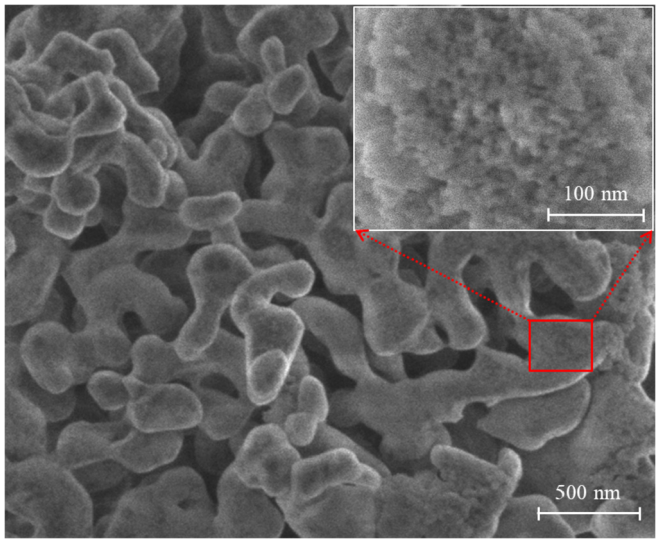

Fig. 6. The SEM images of PANI.

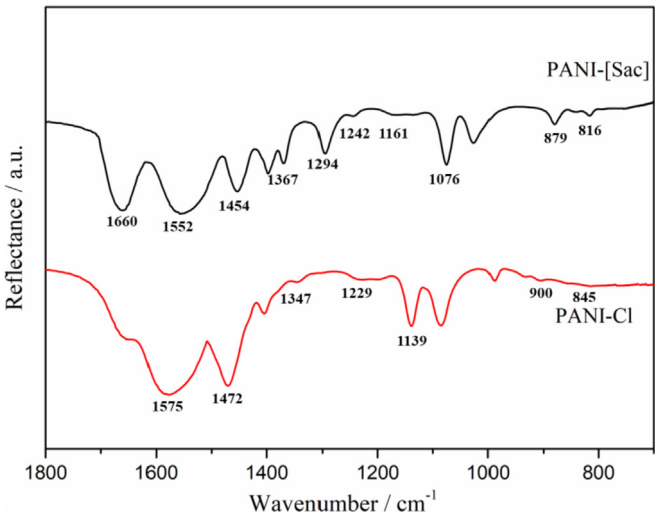

Fig. 7. FTIR spectra of the PANI-[Sac] (black) and PANI-Cl (red) recorded in an ATR mode.
A detachable GC electrode (3 mm in diameter) was used for depositing PANI.

3.5. Electrochemical characterization of PANI

The PANI prepared according to the present strategy was characterized in 1.0 M H_2SO_4 aqueous solution. Fig. 8 is the cyclic voltammogram (2nd cycle) of the resulting PANI. For comparison, Fig. 8 also shows the cyclic voltammogram (2nd cycle) of the PANI prepared according to the conventional strategy (*i.e.* PANI was electrosynthesized in 0.1 M HCl aqueous solution using aniline as monomer with the same deposition charge of ~39.4 mC cm^{-2}). It is seen that the integrated areas of the cyclic voltammograms (*i.e.* the specific capacitance) are almost equal, indicating that the PANI prepared according to the present strategy is comparable to that prepared according to the conventional strategy [26,29].

3.6. Determination of the doping degree of PANI with saccharinate anions

On the electrode surface the aniline monomer is oxidized to form PANI. When PANI is oxidized, $[Sac]^-$ is doped into PANI

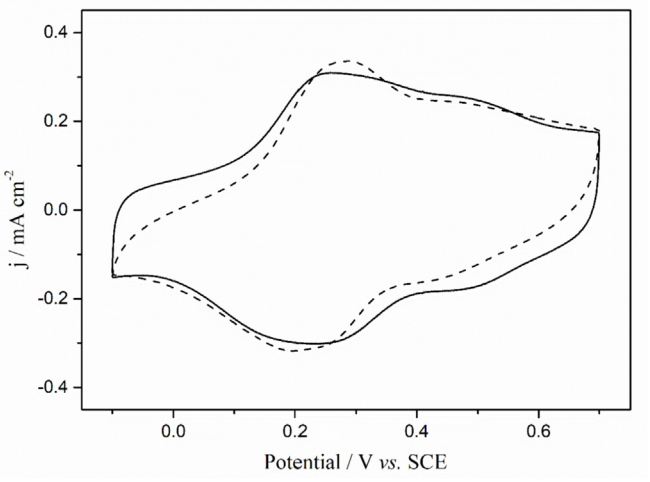

Fig. 8. Cyclic voltammograms (2nd cycle) of PANI prepared with [HANI][Sac] in acetonitrile (solid line) and with ANI in 0.1 M HCl aqueous solution (dashed line) (the deposition charges are both equal). The supporting electrolyte is 1.0 M H_2SO_4 aqueous solution. The potential window is over −0.1–0.7 V. The scan rate is 50 mV s^{-1}.

according to the following equation:

$$m\mathrm{ANI} + \gamma\mathrm{m}[\mathrm{Sac}]^- \rightarrow \left[(ANI)_m^{(\gamma\mathrm{m})+}, \gamma\mathrm{m}[\mathrm{Sac}]^-\right] + 2(m-1)H^+ + (\times (2+\gamma)m - 2)e^- \quad (1)$$

Where γ denotes the doping degree of PANI.

The doping anion ($[Sac]^-$) contains sulfur element while PANI does not, so the percentage of sulfur atoms (S%) determined by EDS could be used to evidence $[Sac]^-$ incorporation into PANI film and the doping degree can be estimated by the following equation (the 15 and the 16 are the atom numbers of $[HANI]^+$ (C_6H_8N) and $[Sac]^-$ ($C_7H_4O_3NS$) [5]:

$$\gamma = \frac{15}{1/(\mathrm{S}\%) - 16} \quad (2)$$

To distinguish between $[Sac]^-$ as a dopant and [Sac] absorbed on the surface of PANI, a control experiment without electrical stimulus was carried out. It was found that the content of $[Sac]^-$ in the PANI decreased from the initial value of 0.386 to the final value of 0.335 when the PANI was immersed in PBS for 175 min. This result indicates that there exists the non-electrostatic adsorption of $[Sac]^-$. Table 1 lists the estimated doping degree of PANI with $[Sac]^-$ under different electrical stimulus conditions. It is seen that the final doping degree decreases with the negative shift of the applied potential; *i.e.*, the larger the driving force the more the drug released [5].

3.7. In vitro electrochemically controlled drug release kinetics

When the PANI film is electrochemically reduced, the anions doped into the PANI film during the electropolymerization is released from PANI film (dedoping). Therefore, the active pharmaceutical ingredients can be released in a controlled way from the conducting polymer carrier by applying different potentials. Based on this rationale, we investigated the *in vitro* drug release kinetics of the PANI-[Sac] film under different applied potentials with the release kinetics without electrical stimulus as control.

Table 1
Estimated final doping degree (γ_f) after electrical stimulus for 175 min.

Applied potential *vs* SCE/V	−0.5	−1.0	−1.5
γ_f	0.125 ± 0.010	0.090 ± 0.007	0.043 ± 0.006

Fig. 9 shows the release of $[Sac]^-$ under different potential stimuli conditions. Without electrical stimulus few $[Sac]^-$ was released (*ca.* 0.2 mmol g^{-1} at the initial stage) [5]. Under electrical stimuli conditions, the amount of drug released (q) increased significantly with time, and at a fixed time, q increased with the negative shift of the applied potential. The above result indicates that the dedoping of the PANI-[Sac] film takes place under negative potential conditions, and the more negative the applied potential, the larger the driving force, the faster the release rate. The maximum q value at −1.5 V is as high as 3.6 mmol g^{-1}. For $[Sac]^-$, this value is higher than that reported in the literature under similar release conditions [5], which is mainly due to the hierarchical porous structure of the present PANI.

To further investigate the release of $[Sac]^-$ from the PANI film, we used the following model to analyze the drug release kinetics [5]:

$$\frac{M_t}{M_0} = kt^n \quad (3)$$

where M_t is the amount of drug released at time t, M_0 is the amount of drug loaded in PANI film, k is a rate constant, t is release time, n is a diffusion exponent related to the diffusion mechanism.

Table 2 lists the kinetic parameters (k and n) of the drug release process based on the plot of ln (M_t/M_0) versus ln(t). It can be seen that without electrical stimulus, n value is close to 0.4, indicating that the release kinetics is in a diffusion mode; under an electrical stimulus the n value is in the range of 0.696–0.765, indicating that the release kinetics is in an anomalous transport mode, which can be attributed to the superposition of diffusion and swelling controlled drug release [5]. The rate constant k under electrical stimulus is higher than that without electrical stimulus, and as the applied potential shift negatively (driving force increases), k increases, indicating that the electrical stimulus could improve the rate of drug release.

3.8. Polymerization charge and the amount of drug released

The amount of drug released is related to the mass of conducting polymer film. For this reason, we investigated the release of $[Sac]^-$ from the PANI-[Sac] films of different masses, which was obtained

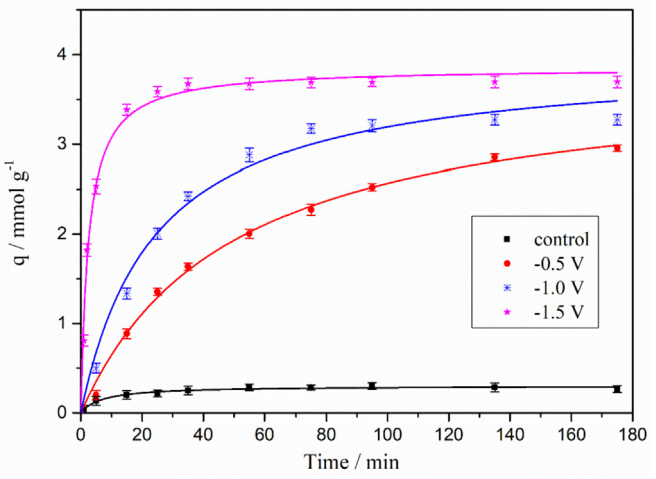

Fig. 9. The release kinetics curves of PANI-[Sac] films under. −0.5 V, −1.0 V and −1.5 V (*vs.* SCE) and without stimulus.

Table 2
Kinetic constant k and diffusion exponent n of PANI-[Sac] film.

Applied potential *vs* SCE/V	K min^{-1}	n	R^2
without stimulus	0.015	0.397	0.999
−0.5 V	0.021	0.696	0.997
−1.0 V	0.038	0.760	0.989
−1.5 V	0.129	0.765	0.992

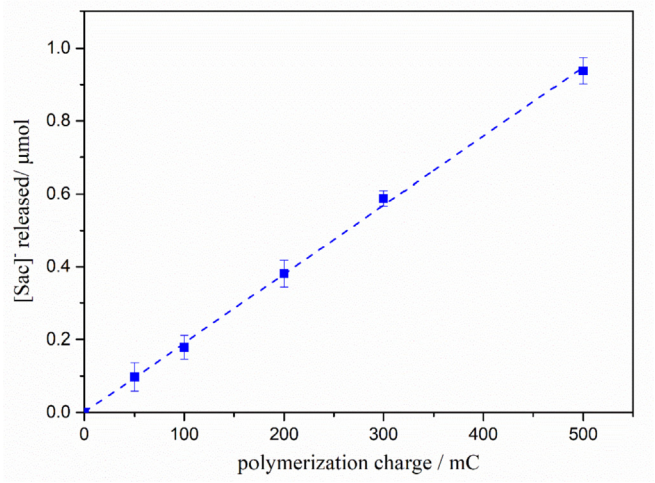

Fig. 10. The amount of drug released under −1.5 V for 150 min for PANI-[Sac] films polymerized at different amounts of charges.

by varying the charges for the electropolymerization. As shown in Fig. 10, the amount of $[Sac]^-$ released at an applied potential of −1.5 V is directly proportional to the polymerization charge [4]. The result indicates that the more the charge for the polymerization, the thicker the PANI film, and the more the amount of drug loaded. The linear relationship also indicates that the PANI-[Sac] drug delivery systems prepared over the charge range of 50−500 mC have a similar release mechanism.

4. Conclusions

In the present work, a novel functionalized organic salt – anilinium saccharinate ([HANI][Sac]) was prepared via ion exchange. In acetonitrile, [HANI][Sac] can be used as monomer as well as supporting electrolyte for efficient electrosynthesis of PANI. The obtained PANI has good electrochemical activity. The doping degree of the resulting PANI with $[Sac]^-$ is as high as 33.5% due to its hierarchical porous structure. The release kinetics of $[Sac]^-$ from the PANI-[Sac] film under different applied potentials indicates that, at the given release time, the release rate and the percentage of $[Sac]^-$ released increase with the negative shift of the applied potential. Moreover, the amount of $[Sac]^-$ loaded and/or released can be regulated by varying the charges for the electropolymerization. The release kinetics also indicates that without electrical stimulus the release process is in a diffusion mode and under electrical stimulus conditions it is in an anomalous transport mode. The present new strategy is helpful for the facile construction of conducting polymer-based electrochemically controlled drug delivery system.

Acknowledgements

We are grateful for the financial support from the National Natural Science Foundation of China (21773143) and the Provincial Key R & D Project of Shandong (2019GSF107090).

References

[1] Z. Wang, X. Deng, J. Ding, W. Zhou, X. Zheng, G. Tang, Mechanisms of drug release in pH-sensitive micelles for tumour targeted drug delivery system: a review, Int. J. Pharm. 535 (2018) 253−260.
[2] K.E. Uhrich, S.M. Cannizzaro, R.S. Langer, K.M. Shakesheff, Polymeric systems for controlled drug release, Chem. Rev. 99 (1999) 3181−3198.
[3] D.G. Kanjickal, S.T. Lopina, Modeling of drug release from polymeric delivery systems - a review, Crit. Rev. Ther. Drug 21 (2004) 345−386.
[4] C. Boehler, F. Oberueber, M. Asplund, Tuning drug delivery from conducting polymer films for accurately controlled release of charged molecules, J. Control. Release 304 (2019) 173−180.
[5] S. Carquigny, B. Lakard, S. Lakard, V. Moutarlier, J.-Y. Hihn, L. Viau, Investigation of pharmaceutically active ionic liquids as electrolyte for the electrosynthesis of polypyrrole and active component in controlled drug delivery, Electrochim. Acta 211 (2016) 950−961.
[6] N. Graf, F. Albertini, T. Petit, E. Reimhult, J. Vörös, T. Zambelli, Electrochemically stimulated release from liposomes embedded in a polyelectrolyte multilayer, Adv. Funct. Mater. 21 (2011) 1666−1672.
[7] X. Luo, X.T. Cui, Sponge-like nanostructured conducting polymers for electrically controlled drug release, Electrochem. Commun. 11 (2009) 1956−1959.
[8] S. Murdan, Electro-responsive drug delivery from hydrogels, J. Control. Release 92 (2003) 1−17.
[9] T.J. Sill, H.A. von Recum, Electrospinning: Applications in drug delivery and tissue engineering, Biomaterials 29 (2008) 1989−2006.
[10] L.L. Miller, Electrochemically controlled release of drug ions from conducting polymers, Mol. Cryst. Liq. Cryst. 160 (1988) 297−301.
[11] N. Alizadeh, E. Shamaeli, Electrochemically controlled release of anticancer drug methotrexate using nanostructured polypyrrole modified with cetylpyridinium: release kinetics investigation, Electrochim. Acta 130 (2014) 488−496.
[12] S. Sankoh, M.Y. Vagin, A.N. Sekretaryova, P. Thavarungkul, P. Kanatharana, W.C. Mak, Colloid electrochemistry of conducting polymer: towards potential-induced in-situ drug release, Electrochim. Acta 228 (2017) 407−412.
[13] E. Shamaeli, N. Alizadeh, Nanostructured biocompatible thermal/electrical stimuli-responsive biopolymer-doped polypyrrole for controlled release of chlorpromazine: kinetics studies, Int. J. Pharm. 472 (2014) 327−338.
[14] S. Geetha, C.R.K. Rao, M. Vijayan, D.C. Trivedi, Biosensing and drug delivery by polypyrrole, Anal. Chim. Acta 568 (2006) 119−125.
[15] R. Wadhwa, C.F. Lagenaur, X.T. Cui, Electrochemically controlled release of dexamethasone from conducting polymer polypyrrole coated electrode, J. Control. Release 110 (2006) 531−541.
[16] J.-M. Pernaut, J.R. Reynolds, Use of conducting electroactive polymers for drug delivery and sensing of bioactive molecules. A redox chemistry approach, J. Phys. Chem. B 104 (2000) 4080−4090.
[17] J. Heinze, B.A. Frontana-Uribe, S. Ludwigs, Electrochemistry of conducting polymers—persistent models and new concepts, Chem. Rev. 110 (2010) 4724−4771.
[18] A.A. Entezami, B. Massoumi, Artificial muscles, biosensors and drug delivery systems based on conducting polymers: a review, Iran. Polym. J. (Engl. Ed.) 15 (2006) 13−30.
[19] B. Zinger, L.L. Miller, Timed release of chemicals from polypyrrole films, J. Am. Chem. Soc. 106 (1984) 6861−6863.
[20] B. Guo, P.X. Ma, Conducting polymers for tissue engineering, Biomacromolecules 19 (2018) 1764−1782.
[21] Y.-x. Sun, K.-f. Ren, Y.-x. Zhao, X.-s. Liu, G.-x. Chang, J. Ji, Construction of redox-active multilayer film for electrochemically controlled release, Langmuir 29 (2013) 11163−11168.
[22] A.J. Heeger, Semiconducting and metallic polymers: the fourth generation of polymeric materials (Nobel Lecture), Angew. Chem. Int. Ed. 40 (2001) 2591−2611.
[23] X. Yu, Y. Sun, L. Xue, X. Huang, Y. Qu, Strategies for improving the catalytic performance of an enzyme in ionic liquids, Top. Catal. 57 (2014) 923−934.
[24] J.P. Hallett, T. Welton, Room-temperature ionic liquids: solvents for synthesis and catalysis, Chem. Rev. 111 (2011) 3508−3576.
[25] T.L. Greaves, C.J. Drummond, Protic ionic liquids: properties and applications, Chem. Rev. 108 (2008) 206−237.
[26] L. Shen, X. Huang, Electrochemical polymerization of aniline in a protic ionic liquid with high proton activity, Synth. Met. 245 (2018) 18−23.
[27] F. Zou, X. Huang, Electropolymerization in proton-functionalized anilinium salts/glycol deep eutectic solvents, J. Mater. Sci. 53 (2018) 8132−8140.
[28] M. Porcher, C. Esnault, F. Tran-Van, F. Ghamouss, Electrochemical deposition and characterization of polypyrrole in electrolyte based on pyrrolidinium hydrogenosulfate protic ionic liquid, J. Appl. Electrochem. 46 (2016) 1133−1145.
[29] G.A. Snook, T.L. Greaves, A.S. Best, A comparative study of the electrodeposition of polyaniline from a protic ionic liquid, an aprotic ionic liquid and neutral aqueous solution using anilinium nitrate, J. Mater. Chem. 21 (2011) 7622−7629.
[30] J. Ding, D. Zhou, G. Spinks, G. Wallace, S. Forsyth, M. Forsyth, D. MacFarlane, Use of ionic liquids as electrolytes in electromechanical actuator systems based on inherently conducting polymers, Chem. Mater. 15 (2003) 2392−2398.

[31] J.L. Shamshina, S.P. Kelley, G. Gurau, R.D. Rogers, Develop ionic liquid drugs, Nature 528 (2015) 188–189.
[32] D. Dobler, T. Schmidts, I. Klingenhöfer, F. Runkel, Ionic liquids as ingredients in topical drug delivery systems, Int. J. Pharm. 441 (2013) 620–627.
[33] R. Ferraz, L.C. Branco, C. Prudêncio, J.P. Noronha, Ž. Petrovski, Ionic liquids as active pharmaceutical ingredients, ChemMedChem 6 (2011) 975–985.
[34] J. Stoimenovski, D.R. MacFarlane, K. Bica, R.D. Rogers, Crystalline vs. ionic liquid salt forms of active pharmaceutical ingredients: a position paper, Pharm. Res. 27 (2010) 521–526.
[35] K. Bica, C. Rijksen, M. Nieuwenhuyzen, R.D. Rogers, In search of pure liquid salt forms of aspirin: ionic liquid approaches with acetylsalicylic acid and salicylic acid, Phys. Chem. Chem. Phys. 12 (2010) 2011–2017.
[36] V. Kumar, S.V. Malhotra, Study on the potential anti-cancer activity of phosphonium and ammonium-based ionic liquids, Bioorg. Med. Chem. Lett 19 (2009) 4643–4646.
[37] W.L. Hough, M. Smiglak, H. Rodríguez, R.P. Swatloski, S.K. Spear, D.T. Daly, J. Pernak, J.E. Grisel, R.D. Carliss, M.D. Soutullo, J.J.H. Davis, R.D. Rogers, The third evolution of ionic liquids: active pharmaceutical ingredients, New J. Chem. 31 (2007) 1429–1436.
[38] L. Viau, C. Tourné-Péteilh, J.-M. Devoisselle, A. Vioux, Ionogels as drug delivery system: one-step sol–gel synthesis using imidazolium ibuprofenate ionic liquid, Chem. Commun. 46 (2010) 228–230.
[39] K. Bica, H. Rodríguez, G. Gurau, O. Andreea Cojocaru, A. Riisager, R. Fehrmann, R.D. Rogers, Pharmaceutically active ionic liquids with solids handling, enhanced thermal stability, and fast release, Chem. Commun. 48 (2012) 5422–5424.
[40] C. Jouannin, C. Tourné-Péteilh, V. Darcos, T. Sharkawi, J.-M. Devoisselle, P. Gaveau, P. Dieudonné, A. Vioux, L. Viau, Drug delivery systems based on pharmaceutically active ionic liquids and biocompatible poly(lactic acid), J. Mater. Chem. B 2 (2014) 3133–3141.
[41] Y. Miwa, H. Hamamoto, T. Ishida, Lidocaine self-sacrificially improves the skin permeation of the acidic and poorly water-soluble drug etodolac via its transformation into an ionic liquid, Eur. J. Pharm. Biopharm. 102 (2016) 92–100.
[42] F. Wang, F. Zou, X. Yu, Z. Feng, N. Du, Y. Zhong, X. Huang, Electrochemical synthesis of poly(3-aminophenylboronic acid) in ethylene glycol without exogenous protons, Phys. Chem. Chem. Phys. 18 (2016) 9999–10004.
[43] E. Mitchell, J. Candler, F. De Souza, R.K. Gupta, B.K. Gupta, L.F. Dong, High performance supercapacitor based on multilayer of polyaniline and graphene oxide, Synth. Met. 199 (2015) 214–218.
[44] H. Karami, M.G. Asadi, M. Mansoori, Pulse electropolymerization and the characterization of polyaniline nanofibers, Electrochim. Acta 61 (2012) 154–164.
[45] D.E. Stilwell, S.M. Park, Electrochemistry of conducting polymers. 2. electrochemical studies on growth properties of polyaniline, J. Electrochem. Soc. 135 (1988) 2254–2262.
[46] P.M.V. Fernandes, J.M. Campiña, N.M. Pereira, C.M. Pereira, F. Silva, Biodegradable deep-eutectic mixtures as electrolytes for the electrochemical synthesis of conducting polymers, J. Appl. Electrochem. 42 (2012) 997–1003.
[47] Y. Wang, Y. Shi, L. Pan, Y. Ding, Y. Zhao, Y. Li, Y. Shi, G. Yu, Dopant-enabled supramolecular approach for controlled synthesis of nanostructured conductive polymer hydrogels, Nano Lett. 15 (2015) 7736–7741.
[48] L. Shen, X. Huang, Tuning the morphologies and electrical properties of azobenzene-4,4′-dicarboxylate-doped polypyrrole via ultraviolet light irradiation and medium pH alteration, Polymer 176 (2019) 188–195.
[49] I. Šeděnková, M. Trchová, J. Stejskal, Thermal degradation of polyaniline films prepared in solutions of strong and weak acids and in water – FTIR and Raman spectroscopic studies, Polym. Degrad. Stab. 93 (2008) 2147–2157.
[50] B.A. Deore, I. Yu, M.S. Freund, A switchable self-doped polyaniline: interconversion between self-doped and non-self-doped forms, J. Am. Chem. Soc. 126 (2004) 52–53.